Water Reduction

DOI: 10.1002/anie.201306504

Water Reduction with Visible Light: Synergy between Optical Transitions and Electron Transfer in Au-TiO_2 Catalysts Visualized by In situ EPR Spectroscopy**

*Jacqueline B. Priebe, Michael Karnahl, Henrik Junge, Matthias Beller, Dirk Hollmann, and Angelika Brückner**

Photocatalytic water splitting by semiconductor catalysts is gaining importance for the sustainable large-scale supply of hydrogen as a major energy carrier.[1] Since its discovery in 1972,[2] this reaction became a hot research topic with the ultimate goal of utilizing sunlight as an abundant energy source. In general, the photocatalytic process is initiated by the excitation of electrons from the valence band into the conduction band of the semiconductor by irradiation with photons of energy equal to or greater than its band gap. One of the most widely used photocatalysts is TiO_2, as it is cheap, environmentally friendly, and shows long-term stability.[3] Unfortunately, pure titania has poor activity for photocatalytic hydrogen production owing to fast electron–hole recombination and/or the large overpotential. Furthermore, TiO_2 is only capable of converting high-energy UV light into chemical energy because of its wide band gap (ca. 3.1 eV). However, for practical applications, catalysts are needed that work efficiently with sunlight, the major part of its radiation being in the visible region. Dedicated synthesis procedures have been applied to shift the absorption edge of TiO_2 into the visible range, for example by doping with other metal cations or anions, but with limited success.[4]

Another promising strategy in activating TiO_2-based photocatalysts for visible-light harvesting is surface coverage by metal nanoparticles owing to their unique optical properties, known as surface plasmon resonance (SPR). This effect implies coherent oscillation of the metal conduction electrons creating an oscillating electric field, which may transfer energy to the semiconductor support. As pointed out in a recent review by Warren and Thimsen as well as by Maldotti et al.,[5] this effect was found to be beneficial for TiO_2-supported coinage metals used for the photoconversion of organic compounds,[6] while its impact on photocatalytic water splitting has not yet been explored in much detail.[7] It is well-known that metal-loaded TiO_2 catalysts show improved activity in photocatalytic water splitting using UV light.[8] This effect has been attributed to an electron transfer from the TiO_2 conduction band to the metal particles, which should suppress recombination of charge carriers (see right part of Figure 1).[9] On the other hand, Silva et al. also

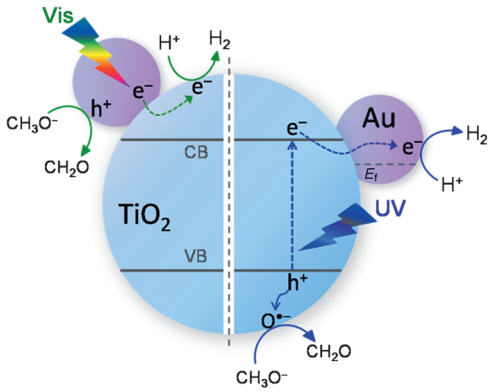

Figure 1. Proposed mechanism for UV- (right) and visible-light (left) driven water reduction using methanol as sacrificial electron donator. CB = conduction band, VB = valence band, h^+ = hole, E_f = Fermi level.

observed an increased H_2 evolution under irradiation of Au-TiO_2 catalysts with monochromatic visible light (λ = 532 nm).[7a] This wavelength is above the TiO_2 absorption edge and coincides more or less with the maximum of the Au-SPR absorption band. Thus, it is plausible to assume that visible light must have been harvested by the gold nanoparticles due to their SPR. However, the mechanism of this absorption as well as its impact on the enhancement of photoactivity in water splitting are not yet fully understood and are controversially discussed. In general, there are two main mechanistic opinions: Gomes Silva et al.[7a] propose an injection of SPR-excited "hot electrons" from the gold particle surface into the TiO_2 conduction band, yet without providing an experimental evidence for this transfer process. Tatsuma and Tian measured an increase of the photocurrent matching exactly the wavelength distribution of the Au SPR band,[10] which was taken as evidence for an electron transfer. However, such improvements in photocurrent have also been explained by changes in light scattering or reflection[11] and not necessarily by electron transfer. Therefore, an increase of photocurrent alone cannot be taken as unequivocal evidence for transfer of electrons from the gold particles to TiO_2.

[*] J. B. Priebe, Dr. M. Karnahl, Dr. H. Junge, Prof. Dr. M. Beller, Dr. D. Hollmann, Prof. Dr. A. Brückner
Leibniz-Institut für Katalyse e.V. an der Universität Rostock
Albert-Einstein-Strasse 29a, 18059 Rostock (Germany)
E-mail: angelika.brueckner@catalysis.de
Homepage: http://www.catalysis.de

[**] This work was supported by the Deutsche Forschungs-gemeinschaft (DFG-SPP1613). We thank Petra Bartels and the service analytical department for their support.

Supporting information for this article is available on the WWW under http://dx.doi.org/10.1002/anie.201306504.

Besides groups favoring the injection of plasmonically oscillating electrons from gold into the TiO_2 conduction band, there are others who claim that this is not possible, as the maxima of the electron injection yield did not match the SPR maximum of gold,[12] and/or individual electrons would not carry enough energy to overcome the ca. 1.1 eV Schottky barrier, because the photon energy is shared by a multitude of electrons.[13] Thus, those groups argue that the SPR effect enhances the local electromagnetic field which in turn initiates electron–hole pair generation within the semiconductor. It has been claimed that this effect is also present even when the noble metal nanoparticles and semiconductors are separated from each other by insulating layers.[14] The above-described state of the art points out that, despite interesting approaches (restricted at present to a few methods only) to unravel the mechanism behind visible-light activity of plasmonic photocatalysts, there still exist different and partly contradicting opinions. This calls for the application of spectroscopic in situ methods providing most reliable information on charge transfer mechanisms and structure–reactivity relationships in working catalysts under reaction conditions. Such knowledge is very important, as it is the basis for rational design of highly efficient plasmonic water-splitting catalysts being an emerging new research field.[5] In this work, we used in situ electron paramagnetic resonance (EPR) spectroscopy for the first time for monitoring water reduction over Au-TiO_2 catalysts with P25 (Degussa) as TiO_2 source consisting of 80% anatase and 20% rutile. This method is ideally suited for visualizing electron-transfer processes under reaction conditions. Its benefits in elucidating reaction mechanisms have recently been demonstrated for homogeneous water reduction using an iridium photosensitizer and an iron carbonyl catalyst.[15]

The catalytic tests in methanol/water mixtures revealed for pure TiO_2 a very small but constant hydrogen production under UV-light irradiation without any loss of activity during 24 h (Table 1; Supporting Information, Figure S2). The H_2 evolution significantly increased after loading gold nanoparticles onto TiO_2. More interestingly, the Au-TiO_2 catalyst enables photocatalytic proton reduction also with pure visible light (400–700 nm), in contrast to the unloaded TiO_2 powder.

To monitor light-induced formation of paramagnetic species, EPR spectra were recorded in the dark and under irradiation with pure visible light (using a cut-off filter >420 nm) and UV/Vis light (without filter), respectively. The spectrum of the as-prepared Au-TiO_2 catalyst in the dark at 90 K exhibits a weak isotropic signal A at $g=2.005$ (Figure 2, Table 2). Such a signal is hardly visible for unloaded TiO_2 (Figure 2, gray lines). We assign it to an electron trapped in an oxygen vacancy,[16] though its g value is slightly higher than usually observed for such species.[16b] This may be due to its close vicinity to Au. Carbon-based radicals, which are also found to respond to light irradiation,[17] can be excluded as origin for signal A because a reference sample prepared without polyvinyl alcohol (PVA) as possible carbon source showed the same signal in almost equal intensity (Supporting Information, Figure S3). Furthermore, signal A decreases and $O_2^{\cdot-}$ is formed when Au-TiO_2 is irradiated in the presence of O_2, indicating electron transfer from species A to O_2 (Supporting Information, Figure S4). A more detailed justification for the assignment of signal A can be found in the Supporting Information.

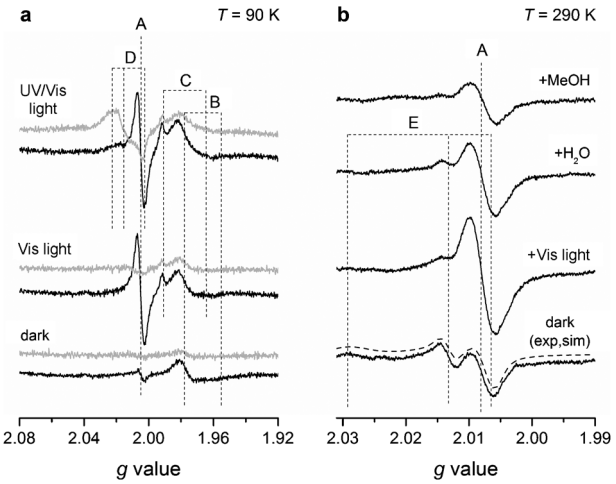

Figure 2. In situ EPR spectra of Au-TiO_2 a) at 90 K compared to pure TiO_2 (gray) in the dark and under pure visible and UV/Vis light; b) in He flow at 290 K in the dark and under visible-light irradiation with subsequent addition of H_2O and methanol. A–E: see text for details.

Furthermore, another weak anisotropic signal B was detected belonging to Ti^{3+} species in the rutile phase of P25 (Figure 2a, Table 2).[18] The corresponding Ti^{3+} signal C in the anatase phase of P25 became well-detectable only under irradiation. Similar signals have also been observed for visible-light-irradiated pure P25, where they have been ascribed to an electron transfer in interwoven rutile and anatase crystallites that form tightly bound nanoclusters.[21] Exclusively in case of the Au-loaded sample, visible-light excitation also led to a strong increase of signal A in the absence of any reactant. Note that the TiO_2 support is not

Table 1: Photocatalytic H_2 evolution of pure and Au-loaded TiO_2 under UV- and visible-light irradiation from MeOH/H_2O mixtures.

Catalyst	Volume V_{H_2} [mL/24 h]		H_2 evolution rate [mmol g^{-1} h^{-1}]	
	UV[a]	Vis[b]	UV[a]	Vis[b]
TiO_2	11	–[c]	0.4	–[c]
Au-TiO_2	875	49	30	1.7

[a] UV = 320–500 nm filter. [b] Vis = 400–700 nm filter. [c] No H_2 detected within detection limits.

Table 2: EPR parameters of detected signals and their assignment based on literature data.

Signal	Assignment	EPR parameters		
		g_1	g_2	g_3
A	e_{cb}^- trapped at O vacancies	2.005	2.005	2.005[16]
B	rutile Ti^{3+}	1.975	1.975	1.951[18]
C	anatase Ti^{3+}	1.990	1.990	1.962[18]
D	Ti^{4+}-$O^{\cdot-}$-Ti^{4+}-OH^-	2.018	2.014	2.004[19]
E	Ti^{4+}-$O_2^{\cdot-}$	2.026	2.010	2.003[20]

capable of absorbing light in this wavelength range. This is clearly evident from the UV/Vis spectrum of TiO_2, the absorption edge of which is located well below 420 nm (Supporting Information, Figure S1). Thus, the trapped electrons reflected by signal A (Figure 2a, middle) might not stem from the TiO_2 valence band, but from the Au nanoparticles. In contrast to TiO_2, the Au nanoparticles are able to absorb visible light, as evident from their absorption band in the UV/Vis spectrum (Figure 4; Supporting Information, Figure S1), which results from a superposition of SPR and d–sp interband absorption features.[22]

We infer that this photoexcitation injects Au electrons into the TiO_2 conduction band, as illustrated in Figure 1 (left hand side). These electrons are then trapped at surface oxygen vacancies in close vicinity to the Au particle/TiO_2 interphase. Such surface defect sites are assumed to be crucial for various heterogeneously catalyzed reactions, as they provide possible binding sites for the reactants. It is known that Au binds preferentially at such oxygen vacancies.[23] Therefore, the photoexcited conduction electrons from Au are likely to be trapped by those defects as well. It must also be stressed that signal **A** cannot arise from electrons located in the gold particles themselves, as such electrons give rise to signals with much higher g values and line width. Thus, a signal at $g = 2.0636$ has been observed at 77 K for Au particles of only 1.4 nm diameter supported on ZrO_2, and it was shown that the peak-to-peak line width rapidly increases with the particle diameter, reaching 1186 G for particles of 5.3 nm size.[24] This means that conduction electron signals of Au particles with a diameter of 10–15 nm such as in the present catalyst would be broadened beyond detection and, thus, not observable by EPR spectroscopy. Interestingly, no signal A is formed when pure TiO_2 is irradiated with visible light in the same way (Figure 2a, middle, gray line). This is another support for its assignment to electron transfer from gold to TiO_2.

By exciting the catalyst at 90 K with the whole wavelength range of the Xe lamp containing also UV light (200–700 nm), electron–hole pair generation may occur within TiO_2, as illustrated in Figure 1 (right hand side). This process is demonstrated on the one hand by an increase of signals B and C, reflecting the formation of Ti^{3+} upon photoexcited electron trapping at Ti^{4+}. On the other hand, a new anisotropic signal D is formed (Figure 2a, Table 2), which, based on literature data,[19] is assigned to $O^{\bullet-}$ radicals resulting from trapping of the positive holes by lattice O^{2-} species at low temperature. In Au-TiO_2 the intensity of signal D is weaker than in pure TiO_2. This may be due to the higher amount of oxygen vacancies in Au-TiO_2, leading to a deficient O^{2-} species available for hole trapping. Similarly, a decrease of the $O^{\bullet-}$ EPR signal has been observed with decreasing crystallinity of TiO_2, which might contain more anionic vacancies than highly crystalline TiO_2.[25]

For analyzing the behavior of light-induced EPR signals under reaction-like conditions to further explore reaction-involved species, in situ EPR spectra at room temperature in the dark as well as during irradiation with visible light under flowing helium subsequently loaded with H_2O and methanol were recorded (Figure 2b). The evolution of hydrogen under light irradiation is evident from on-line mass spectrometry (Supporting Information, Figure S5). The Ti^{3+} signals B and C were not observed at this temperature, which is most likely due to short relaxation times. However, the isotropic signal A was properly seen at $T = 290$ K. Similar to the experiment at 90 K, its intensity increased strongly under visible-light excitation. As mentioned above, this might be due to the injection of electrons from gold to the TiO_2 conduction band followed by trapping at surface oxygen vacancies. Interestingly, this signal lost intensity when water and methanol were added to the catalyst under irradiation, indicating that it is also these electrons which are consumed by reduction of protons to H_2. In any case, the g_2 component of surface-bound $O_2^{\bullet-}$ radicals ($g_1 = 2.026$, $g_2 = 2.010$, and $g_3 = 2.003$)[20] is properly seen in the spectrum (signal E) as confirmed by spectrum simulation (dashed lines in Figure 2b; for parameters, see the Supporting Information). However, this latter species is hardly affected by irradiation.

To further explore the impact of UV and visible light on electron transfer processes in Au-TiO_2, the intensity of the EPR signal (double integral) at room temperature was monitored as a function of time during irradiation at distinct wavelengths of (280 ± 10) nm and (532 ± 10) nm, respectively, in the absence of any reactant by using two band-pass filters (Figure 3). There was hardly any EPR signal detectable during irradiation with pure UV light, which excites electrons from the valence to the conduction band of TiO_2 (Figure 1, right hand side). This might be due to the fact that at 290 K those excited electrons are rapidly transferred to the Au particle with lower Fermi level prior to being trapped at Ti^{4+} species or oxygen vacancies. For reasons explained above, no EPR signal can be observed for Au conduction electrons. When switching from 280 to 532 nm, signal **A** rapidly increases and declines again when light is shut off (Figure 3a). For the formation and decline processes, time constants τ_f and

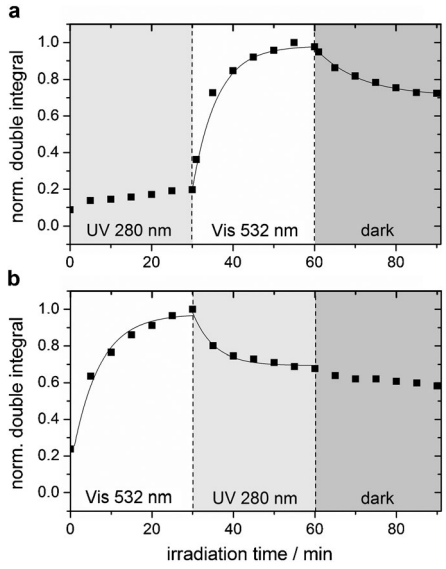

Figure 3. Double integrals of the EPR signal A (symbols) and kinetic fits (lines, for details see Supporting Information) as a function of irradiation time at 290 K starting with UV and switching to visible light after 30 min (a) and vice versa (b).

τ_{dec} have been derived by fitting the time dependence of the EPR signal intensity (double integrals) using exponential approximation equations (solid lines in Figure 3; for details, see the Supporting Information, Table S3). The τ values indicate how fast the formation or decay of the EPR signal occurs. It was found that trapping of electrons under visible light (reflected by rising intensity of signal **A**) proceeds in the same time, regardless the fact whether the sample was kept before under UV light (Figure 3a, $\tau_f = 6.0$ min) or in the dark (Figure 3b, $\tau_f = 6.5$ min). In contrast, the decay time constants are markedly different in both experiments: When light is shut off after irradiation at 532 nm, the decay is much slower (Figure 3a, $\tau_{dec} = 10.9$ min) in comparison to the second experiment (Figure 3b, $\tau_{dec} = 5.3$ min), in which just the irradiation wavelength was changed from 532 to 280 nm. Obviously, a UV-stimulated back-transfer of the trapped electrons into the Au conduction band (where they are not detectable by EPR) occurs under these conditions, instead of a slow relaxation mechanism observed in the first case. This is also supported by an experiment in which the sample was first exposed to visible light only (using a cut-off filter > 420 nm) followed by irradiation with the full wavelength range after removal of the cut-off filter, which led to a significant signal intensity loss (Supporting Information, Figure S6).

To investigate whether visible-light-induced electron transfer is related to the Au surface plasmon resonance, the formation of signal **A** has been studied under irradiation with light of different but defined wavelengths using a set of band pass filters. The double integral of the EPR signal is plotted together with the SPR band of the catalyst in Figure 4. The corresponding EPR spectra are shown in the Supporting Information, Figure S7a. Starting at 300 nm, the irradiation wavelength was kept constant for 15 min before switching stepwise to the next higher wavelength up to 700 nm. The curve exhibits a maximum at excitation wavelengths of 450 to 500 nm, which is in good agreement with the maximum value for the wavelength-dependent electron injection yield measured by Du et al.[12] They distinguished two different electron injection pathways, which were assigned to direct electron–hole pair generation by d–sp interband transition in the shorter wavelength region, respectively to a plasmon-induced enhancement of the electromagnetic field at higher wavelengths (> 580 nm). Both effects are also supported by our wavelength dependent measurements (Figure 4; Supporting Information, Figure S7), in which an intensity growth of signal **A** upon lowering the wavelengths from 700 nm to 550 nm was observed that parallels almost exactly the slope of the Au SPR band (Supporting Information, Figure S7b). The additional intensity increase below 550 nm cannot be explained by SPR promotion but might be supported by the interband transition of the Au electrons.

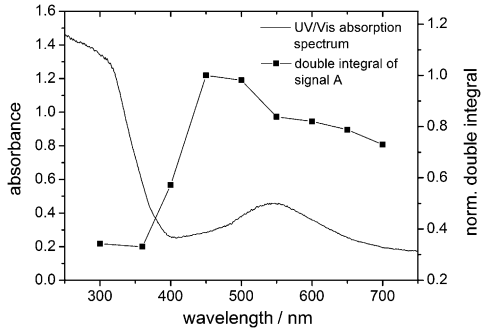

Figure 4. Double integrals of the EPR signal A (symbols) as a function of irradiation wavelength in comparison to the SPR absorption band of Au-TiO_2.

In summary, we have directly monitored visible-light-driven electron transfer for the first time from the Au conduction band to the TiO_2 support surface where they are trapped in vacancies in close vicinity to the Au-TiO_2 interphase. This was possible by monitoring Au-TiO_2 catalysts during photocatalytic water reduction with light of different, but distinct wavelength, using in situ EPR spectroscopy, which is a unique technique to selectively visualize unpaired electrons. The results suggest that depending on the wavelength, this electron transfer is stimulated by the joint action of two different electron excitation pathways within the Au particle, namely d–sp interband transitions in the lower and SPR transitions in the higher wavelength range of the visible spectrum. It is anticipated that the visible-light harvesting capability of supported Au photocatalysts can be improved even more when future efforts in catalyst development are focused on shifting the absorption edge energy of the semiconductor support towards the range in which Au electrons can be excited.

Experimental Section

The Au(1.0 wt%)-TiO_2 powder photocatalyst was prepared by sol immobilization as described previously.[26] Briefly, PVA (1.2 mL, 1 wt% solution, Merck Chemicals) was added to a solution of $HAuCl_4 \cdot 3H_2O$ (20 mg) in distilled water (5 mL). A dark sol was formed by adding dropwise a freshly prepared $NaBH_4$ solution (2.5 mL, 0.1M, Aldrich, $> 96\%$). After 30 min, TiO_2 (1.0 g, P25 Degussa) was added and the suspension further stirred for 12 h at room temperature. The precipitate was washed with 500 mL distilled water and dried at 100°C for 12 h. Au particles on TiO_2 with diameters of about 10–15 nm were obtained (Supporting Information, Figure S8).

All catalytic experiments were carried out under an argon atmosphere with freshly distilled solvents (conditions: 50 mg catalyst, 10 mL MeOH/H_2O (1:1), 7.2 W Hg vapor light irradiation, $T = 25$°C, $t = 24$ h). Further details on the equipment and the experimental set-up have been reported previously.[27]

UV/Vis spectra were recorded by an Avantes AvaSpec-2048 UV/Vis spectrometer via an Avantes 45° optical probe. For details of the X-band EPR measurements, see the Supporting Information.

Received: July 25, 2013
Revised: August 26, 2013
Published online: September 12, 2013

Keywords: electron transfer · EPR spectroscopy · surface plasmon resonance · water splitting

[1] a) M. Ni, M. K. H. Leung, D. Y. C. Leung, K. Sumathy, *Renewable Sustainable Energy Rev.* **2007**, *11*, 401–425; b) N. Armaroli, V. Balzani, *Angew. Chem.* **2007**, *119*, 52–67; *Angew. Chem. Int. Ed.* **2007**, *46*, 52–66.

[2] A. Fujishima, *Nature* **1972**, *238*, 37 – 38.
[3] M. R. Hoffmann, S. T. Martin, W. Choi, D. W. Bahnemann, *Chem. Rev.* **1995**, *95*, 69 – 96.
[4] a) W. Choi, A. Termin, M. R. Hoffmann, *J. Phys. Chem.* **1994**, *98*, 13669 – 13679; b) H. Irie, Y. Watanabe, K. Hashimoto, *J. Phys. Chem. B* **2003**, *107*, 5483 – 5486.
[5] a) S. C. Warren, E. Thimsen, *Energy Environ. Sci.* **2012**, *5*, 5133 – 5146; b) A. Maldotti, A. Molinari, R. Juárez, H. Garcia, *Chem. Sci.* **2011**, *2*, 1831 – 1834.
[6] a) B. K. Min, J. E. Heo, N. K. Youn, O. S. Joo, H. Lee, J. H. Kim, H. S. Kim, *Catal. Commun.* **2009**, *10*, 712 – 715; b) S. T. Kochuveedu, D.-P. Kim, D. H. Kim, *J. Phys. Chem. C* **2012**, *116*, 2500 – 2506.
[7] a) C. Gomes Silva, R. Juárez, T. Marino, R. Molinari, H. García, *J. Am. Chem. Soc.* **2011**, *133*, 595 – 602; b) J. J. Chen, J. C. S. Wu, P. C. Wu, D. P. Tsai, *J. Phys. Chem. C* **2011**, *115*, 210 – 216.
[8] a) H. Liu, J. Yuan, W. Shangguan, *Energy Fuels* **2006**, *20*, 2289 – 2292; b) G. R. Bamwenda, S. Tsubota, T. Nakamura, M. Haruta, *J. Photochem. Photobiol. A* **1995**, *89*, 177 – 189.
[9] J. Sá, M. Fernández-García, J. A. Anderson, *Catal. Commun.* **2008**, *9*, 1991 – 1995.
[10] Y. Tian, T. Tatsuma, *J. Am. Chem. Soc.* **2005**, *127*, 7632 – 7637.
[11] R. Solarska, A. Królikowska, J. Augustyński, *Angew. Chem.* **2010**, *122*, 8152 – 8155; *Angew. Chem. Int. Ed.* **2010**, *49*, 7980 – 7983.
[12] L. Du, A. Furube, K. Hara, R. Katoh, M. Tachiya, *J. Photochem. Photobiol. C: Photochem. Rev.* **2013**, *15*, 21 – 30.
[13] E. W. McFarland, J. Tang, *Nature* **2003**, *421*, 616 – 618.
[14] a) D. B. Ingram, S. Linic, *J. Am. Chem. Soc.* **2011**, *133*, 5202 – 5205; b) S. K. Cushing, J. Li, F. Meng, T. R. Senty, S. Suri, M. Zhi, M. Li, A. D. Bristow, N. Wu, *J. Am. Chem. Soc.* **2012**, *134*, 15033 – 15041.
[15] D. Hollmann, F. Gärtner, R. Ludwig, E. Barsch, H. Junge, M. Blug, S. Hoch, M. Beller, A. Brückner, *Angew. Chem.* **2011**, *123*, 10429 – 10433; *Angew. Chem. Int. Ed.* **2011**, *50*, 10246 – 10250.
[16] a) I. Nakamura, N. Negishi, S. Kutsuna, T. Ihara, S. Sugihara, K. Takeuchi, *J. Mol. Catal. A* **2000**, *161*, 205 – 212; b) S. O. Baumann, M. J. Elser, M. Auer, J. Bernardi, N. Hüsing, O. Diwald, *Langmuir* **2011**, *27*, 1946 – 1953.
[17] E. A. Konstantinova, A. I. Kokorin, S. Sakthivel, H. Kisch, K. Lips, *Chimia* **2007**, *61*, 810 – 814.
[18] M. Okumura, J. M. Coronado, J. Soria, M. Haruta, J. C. Conesa, *J. Catal.* **2001**, *203*, 168 – 174.
[19] a) T. Hirakawa, H. Kominami, B. Ohtani, Y. Nosaka, *J. Phys. Chem. B* **2001**, *105*, 6993 – 6999; b) C. P. Kumar, N. O. Gopal, T. C. Wang, M.-S. Wong, S. C. Ke, *J. Phys. Chem. B* **2006**, *110*, 5223 – 5229.
[20] R. F. Howe, M. Grätzel, *J. Phys. Chem.* **1987**, *91*, 3906 – 3909.
[21] D. Hurum, A. Agrios, S. Crist, K. Gray, T. Rajh, M. Thurnauer, *J. Electron Spectrosc.* **2006**, *150*, 155 – 163.
[22] K. Ueno, H. Misawa, *J. Photochem. Photobiol. A* **2011**, *221*, 130 – 137.
[23] J. Zhang, G. Chen, M. Chaker, F. Rosei, D. Ma, *Appl. Catal. B: Environ.* **2013**, *132 – 133*, 107 – 115.
[24] P. Claus, A. Brückner, C. Mohr, H. Hofmeister, *J. Am. Chem. Soc.* **2000**, *122*, 11430 – 11439.
[25] N. O. Gopal, H.-H. Lo, T.-F. Ke, C.-H. Lee, C.-C. Chou, J.-D. Wu, S.-C. Sheu, S. C. Ke, *J. Phys. Chem. C* **2012**, *116*, 16191 – 16197.
[26] N. Dimitratos, J. A. Lopez-Sanchez, D. Morgan, A. Carley, L. Prati, G. J. Hutchings, *Catal. Today* **2007**, *122*, 317 – 324.
[27] F. Gärtner, S. Losse, A. Boddien, M. M. Pohl, S. Denurra, H. Junge, M. Beller, *ChemSusChem* **2012**, *5*, 530 – 553.

